SPEMT imaging with a dedicated VAoR dual-head camera: preliminary results

2009 JINST 4 P10012

(http://iopscience.iop.org/1748-0221/4/10/P10012)

Jinst

PUBLISHED BY IOP PUBLISHING FOR SISSA

RECEIVED: *September 1, 2009*
ACCEPTED: *October 1, 2009*
PUBLISHED: *October 28, 2009*

SPEMT imaging with a dedicated VAoR dual-head camera: preliminary results[1]

M. Camarda,[a,2] N. Belcari,[a] A. Del Guerra,[a] S. Vecchio,[a] P. Bennati,[b] M.N. Cinti,[b] R. Pani,[b] R. Campanini,[c] E. Iampieri[c] and N. Lanconelli[c]

[a] *Department of Physics "E. Fermi", University of Pisa and INFN Pisa, Pisa I-56124, Italy*

[b] *Department of Experimental Medicine and Pathology, University of Rome "La Sapienza", Rome I-00100, Italy*

[c] *Department of Physics, University of Bologna, Bologna, Italy*

E-mail: manuela.camarda@pi.infn.it

ABSTRACT: We have developed a SPEMT (Single Photon Emission MammoTomography) scanner that is made up of two cameras rotating around the pendulous breast of the prone patient, in Vertical Axis of Rotation (VAoR) geometry. Monte Carlo simulations indicate that the device should be able to detect tumours of 8 mm diameter with a tumour/background uptake ratio of 5:1. The scanner field of view is 41.6 mm height and 147 mm in diameter. Each head is composed of one pixilated NaI(Tl) crystal matrix coupled to three Hamamatsu H8500 64-anodes PMT's read out via resistive networks. A dedicated software has been developed to combine data from different PMT's, thus recovering the dead areas between adjacent tubes. A single head has been fully characterized in stationary configuration both in active and dead areas using a point-like source in order to verify the effectiveness of the readout method in recovering the dead regions. The scanner has been installed at the Nuclear Medicine Division of the University of Pisa for its validation using breast phantoms. The very first tomographic images of a breast phantom show a good agreement with Monte Carlo simulation results.

KEYWORDS: Gamma camera, SPECT, PET PET/CT, coronary CT angiography (CTA); X-ray mammography and scinto- and MRI-mammography

[1] This work was partially supported by the MIUR, in the framework of the PRIN2004 program, number 2004028450, and by the Network of Excellence European Molecular Imaging Laboratories (EMIL) grant LSHC-CT-2004-503569.

[2] Corresponding author, now at Servizio di Fisica Medica, Ospedale S. Lucia, Macerata, Italy.

doi:10.1088/1748-0221/4/10/P10012

2009 JINST 4 P10012

Contents

2009 JINST 4 P10012

1 Introduction

Nuclear medicine imaging techniques (PET and SPECT) in breast cancer investigation provide functional information that can be complementary to anatomical information obtained with standard mammography. In the past years dedicated cameras with a small field-of-view [] have been developed to overcome the limitations of clinical scanners that show poor spatial resolution in detecting small size breast lesions.

We have developed a Single Photon Emission MammoTomography (SPEMT) scanner having two heads which revolve around the pendulous breast of the prone patient. Vertical Axis of Rotation (VAoR) geometry improves resolution by minimizing the radius of rotation. Also, since the patient is in prone position, the thorax is kept away from the field-of-view, thus reducing the scatter radiation from heart and liver. Monte Carlo simulations have been made for the system optimization and for the evaluation of the detector performances.

Simulation results indicate that tumours of 8 mm diameter are detectable with a tumour/background uptake ratio of 5:1 [], thus overcoming the present clinical sensitivity limit (about 1 cm diameter) for the detection of small tumours [].

2 SPEMT tomograph

The proposed SPEMT scanner has two opposing detector heads of approximately 5×15 cm^2 each, with a system field-of-view of 147 mm $\emptyset$ and 41.6 mm height. The radius of rotation is 7.0 cm thus enabling breasts up to 14 cm in diameter to be scanned. Each head is composed of a pixelated

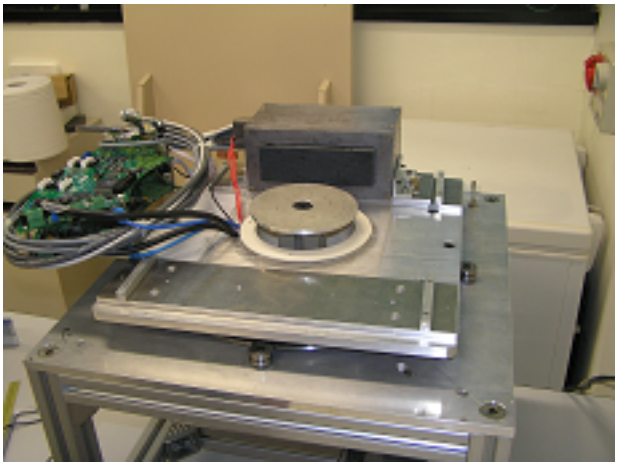

Figure 1. The SPEMT scanner equipped with a single head. The round device is the source holder.

NaI(Tl) crystal matrix (2.2 mm pitch, 6 mm thickness) with a 3 mm thick glass window coupled to three Hamamatsu H8500 64-anodes PMT's. A parallel hole lead collimator (22 mm thick, with 1.5 mm holes and 0.2 mm septa) is placed in front of the matrix. A picture of the SPEMT scanner with one head installed is shown in figure 1.

Since each head has 3×8×8 outputs, a multiplexed readout has been implemented in order to obtain a system easy to be handled in a clinical environment. For the read out of each Multi Anode PMT, a Symmetric Charge Division (SCD) [] resistive chain is used to reduce the number of signals from 8×8 to 8+8. As a second stage non-conventional resistive chains, working as analogue converters [], are implemented to further reduce the number of signals to 4. Dedicated electronics boards perform digitization and acquisition of the 3×4 signals from each head. The digital data are sent to a local PC server via USB2 connection.

3 Methods and measurements

When tiling two or more PMT's to have a wider detector, dead zones in between can't be avoided. In this case the effective dead area is about 8 mm between each pair of adjacent PMT's. The light from those events firing the crystals in front of this area is spread out by the glass windows (3 mm thick matrix window + 1.5 mm thick H8500 window) producing detectable signals in both contiguous MAPMT's. Dedicated electronic boards have been developed to provide time correlation tags on event signals. The dedicated software combines time correlated data from adjacent MAPMT's, thus recovering the dead areas.

3.1 Detector characterization

One single head has been fully characterized in stationary configuration in both active and dead areas, using a ^{57}Co point like sealed source (122 keV).

Flood-field measurements (without collimator) have been performed to test the pixel identification capability of the detector and to evaluate the energy resolution. Planar images of the point like source were acquired at increasing Source-to-Detector Distances (SDD) both in the active and

2009 JINST 4 P10012

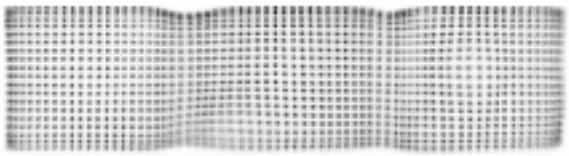

Figure 2. Flood-field irradiation of the single head (without collimator) with a ^{57}Co point like source (122 keV).

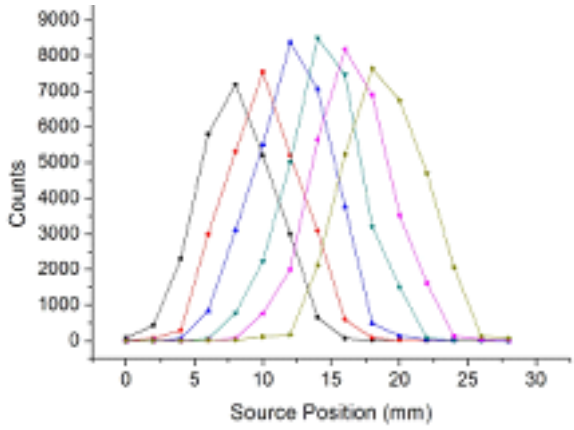

Figure 3. System spatial resolution measurements at SDD=6 mm obtained by moving a ^{57}Co point like source along a line parallel to the collimator plane; each curve corresponds to a fixed position of the source.

in the recovered regions. Spatial resolution in planar images and system sensitivity have been estimated. Intrinsic spatial resolution has been evaluated by moving the source along a line parallel to the collimator plane, with a step size of 2 mm and a SDD of 6 mm.

3.2 Tomograph calibrations

Detector calibration procedure is implemented in the dedicated software, including gain alignment, sensitivity normalization, data acquisition dead time and radionuclide decay corrections.

To perform sensitivity correction, a planar phantom, uniformly filled with 111MBq of ^{99m}Tc, was used.

3.3 Tomographic acquisitions

A home made breast phantom was built consisting of a cylinder of 9 cm Ø, 13 cm height filled with an aqueous solution of ^{99m}Tc. A small cylinder of 8 mm Ø, 5 mm height was placed at the centre of the phantom mimicking a tumour. Acquisitions were performed in clinical conditions with a background concentration of 100nCi/cc and an acquisition time of 20 minutes equivalent (40 minutes with one head). The tumour to background ratio was set at 10:1 and 5:1.

Tomographic images were reconstructed using an iterative method based on a simulated annealing technique. 2D slices are composed of 67×67 pixels, with a voxel side equal to 2.2 mm.

Table 1. Planar image spatial resolution at different SDD.

SDD	0.5cm	3.0cm	6.0cm
Active area	2.5mm	4.3mm	5.8mm
Recovered area	2.6mm	4.7mm	6.8mm

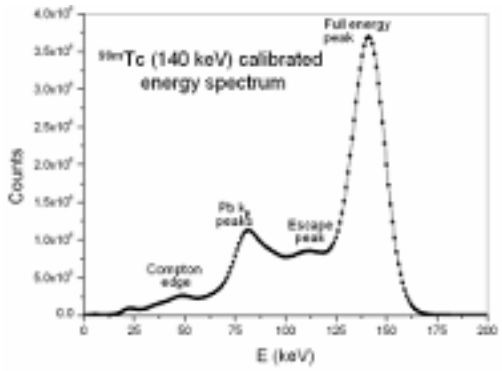

Figure 4. ^{99m}Tc calibrated energy spectrum of a planar phantom.

4 Results

4.1 Detector characterization

Flood-field irradiation of a single head (without collimator) shows that all the crystals of the pixilated NaI(Tl) matrix are clearly distinguishable (figure 2). The average peak-to-valley ratio is about 4. The energy resolution at 122 keV is 14% in the active area and 16% in the recovered zone.

The values of spatial resolution in planar images measured using the ^{57}Co point like source at different SDD are reported in table 1. The spatial resolution extrapolated to SDD = 0 cm is 2.2 mm FWHM.

The sensitivity measured with the ^{57}Co source of 1.5 MBq for a SDD of 6 mm is 140 cps/MBq in both regions.

The system spatial resolution of the detector head, measured at SDD = 6 cm, is shown in figure 2. Different curves correspond to different fixed position of the source. For every position the counts in each crystal are plotted. The average spatial resolution is 6.7 mm FWHM.

4.2 Tomograph calibration

The stationary head was flood field irradiated with ^{99m}Tc; the average Peak-to-Valley ratio is 5.2 and the spatial resolution is 1.1mm FWHM.

Figure 3 shows the calibrated spectrum, with gain correction applied. Energy resolution is 13% at 140 keV. The number of counts in each pixel in the 132 keV–156 keV energy window were used to perform efficiency normalization.

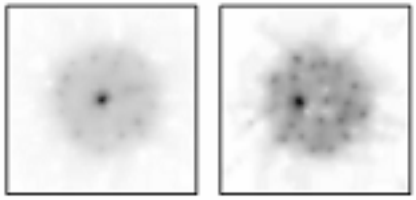

Figure 5. Reconstructed transaxial slices of 8 mm tumour in the 9 cm thick breast phantom with T/B equal to 10:1 (left) and 5:1 (right).

Table 2. SNR values calculated from simulated and measured data.

T/B	**10:1**	**5:1**
Simulated SNR	9	6.5
Measured SNR	8.5	6.3

4.3 Tomographic acquisitions

Tomographic reconstructions of the central slice of the breast phantom containing the 8 mm tumour are shown in Table 1, for T/B=10:1 and T/B=5:1.

Signal to Noise Ratio (SNR) was calculated for reconstructed transaxial slices according to the following equation:

$$SNR = \frac{\Sigma_{\mathrm{ROI}} - BKG}{\sigma_{\mathrm{BKG}}} \tag{4.1}$$

where Σ_{ROI} is the mean over a ROI centered on the tumour; BKG and σ_{BKG} are the mean and the standard deviation of background, respectively. The region of interest over the hot detail was 3×3 pixels wide centered on the maximum count. For the background calculation a region 9×9 pixels wide around the tumour was excluded, in such a way that pixels in the periphery of the hot detail do not influence the background counts.

The SNR values were compared with those obtained from Monte Carlo simulations. In this case the breast phantom was a cylinder of 8 cm Ø and 8 cm height with a spherical tumour of 8 mm Ø. Results are shown in table 2.

5 Conclusions

One single head of the SPEMT tomograph has been characterized. Measurements show good agreement with Monte Carlo simulations and verify the effectiveness of the readout method in recovering the dead regions. A dedicated software was developed for calibration, including gain alignment, sensitivity normalization, data acquisition dead time and radionuclide decay corrections.

The scanner with a single head has been installed at the Nuclear Medicine Division of the University of Pisa for its validation using breast phantoms. The first tomographic images of a home made breast phantom, filled with ^{99m}Tc, showed that the SPEMT scanner is able to detect 8 mm tumours having a T/B=5:1 with an SNR=6.3, in agreement with previous Monte Carlo simulations.

2009 JINST 4 P10012

References

[1] M. Camarda et al., *Development of the YAP-PEM scanner for breast cancer imaging*, *Phys. Med.* **21S1** (2006) 114.

[2] G.K. Loudos et al., *High-resolution and high-sensitivity SPECT imaging of breast phantoms* , *Nucl. Instrum. Meth.* **A 527** (2004) 97.

[3] N. Lanconelli et al., *Conference records of* 2006 *IEEE NSS/MIC/RTSD*, San Diego U.S.A. (2006).

[4] O. Schillaci et al., *Clinical utility of scintimammography: from the Anger-camera to new dedicated devices* , *Nucl. Instrum. Meth.* **A 569** (2006) 281.

[5] P.D. Olcott et al., *Compact readout electronics for position sensitive photomultiplier tubes*, *IEEE Trans. Nucl. Sci.* **52** (2005) 21.

[6] V. Popov et al., *Conference records of* 2001 *IEEE NSS/MIC/RTSD*, IEEE, San Diego U.S.A. (2001).

[7] N. Belcari et al., *Performance of a four-output front-end electronics for multi-anode PMTS readout of scintillator arrays*, *Nucl. Instrum. Meth.* **A 572** (2007) 335.

[8] R. Pani et al., *Custom breast phantom for an accurate tumor SNR analysis*, *IEEE Trans. Nucl. Sci.* **51** (2004) 198.

2009 JINST 4 P10012